Pergamon

0042-6989(95)00139-5

Vision Res., Vol. 36, No. 4, pp. 559–572, 1996

0042-6989/96 $15.00 + 0.00

Second-order Illusions: Mach Bands, Chevreul, and Craik–O'Brien–Cornsweet*

ZHONG-LIN LU,† GEORGE SPERLING†

Received 22 June 1994; in revised form 10 April 1995

Mach bands, which normally occur at the edges of ramp modulations of luminance, are demonstrated to occur in fullwave stimuli that have ramp modulations of contrast while maintaining constant expected luminance. [The fullwave stimuli are random textures that (1) have a ramp contrast modulation that is exposed by fullwave rectification (e.g. absolute value or square) or by halfwave rectification but (2) have a uniform expected luminance throughout, so the the modulation remains hidden without rectification.] Two different textures were used: random pixels and 'Mexican hats'. Stimuli were presented dynamically, with a new instantiation of the texture every 67 msec (this enhances the magnitude of the illusion). Both fullwave Mach-band stimuli exhibit perceptual Mach bands that are decreases or increases in apparent texture *contrast* with no concomitant change in apparent brightness. The perceived *contrast* bands in fullwave Mach stimuli and the *brightness* bands in a conventional luminance Mach-band stimulus have approximately the same magnitude. Chevreul (staircase) illusions in luminance and in fullwave patterns also are found to have approximately similar magnitudes, as do luminance and fullwave Craik–O'Brien–Cornsweet illusions. None of these illusions can be perceived with halfwave textures. These results indicate that second-order (texture) illusions result from *fullwave*, not *halfwave*, rectification and involve spatial interactions that are remarkably similar to those in first-order (luminance) processing.

Texture perception   Illusions   Nonlinear processing   Mach bands   Second-order processing
Fullwave rectification   Halfwave rectification

INTRODUCTION

First-order illusions

When two plateaus of constant luminance are joined by a linear luminance ramp, illusory bands are perceived at the junctions—an induced dark band is perceived at the bottom of the ramp, and a bright band near the top of the ramp [Fig. 1(a, b)]. This illusion was reported by Ernst Mach in the 19th century (Mach, 1865; Ratliff, 1965) and now bears his name. Chevreul illusions (Chevreul, 1890; von Bekesy, 1968; Ross, Holt, & Johnstone, 1981) can be demonstrated with a luminance staircase that increases from step to step [Fig. 1(c, d)]. In the Craik–O'Brien–Cornsweet illusion (Craik, 1940; O'Brien, 1958; Cornsweet, 1970), a concentric black ring and white ring imposed on a uniform surface change the (apparent) brightness of the entire circumscribed area [Fig. 1(e, f)]. In all of these illusions, the spatial distribution of perceived brightness diverges strikingly from the physical distribution of luminance. Although much is known about the complex spatial and spatial-channel interactions in these illusions, none has received a completely satisfactory explanation (e.g. Mach, 1865; Fry, 1948; Huggins & Licklider, 1951; Hartline & Ratliff, 1954; Taylor, 1956; von Bekesy, 1960; Todorovic, 1987; Grossberg & Todorovic, 1988; Ross, Morrone & Burr, 1989; Kingdom & Moulden, 1992; Morrone, Burr & Ross, 1994; Burr, 1987; Burr & Morrone, 1994).

Second-order illusions

In a contrast analog to the well-known Simultaneous Brightness Contrast illusion, Chubb, Sperling and Solomon (1989) demonstrated reduction of the apparent contrast of a textured test patch when the patch was surrounded by a textured area of higher contrast (see also Cannon & Fullenkamp, 1991, 1993; Solomon, Sperling & Chubb, 1993; Singer & D'Zmura, 1994, 1996). {In the original first-order (luminance) illusion, the apparent brightness of a test patch is reduced when it is surrounded by an area of higher luminance [Fig. 1(g, h)].} Phenomena that become apparent when the spatial variation of luminance is replaced with a spatial variation in contrast are called second-order phenomena because

*Research first reported at the annual meeting of the Association for Research in Vision and Ophthalmology, 1993.

†Department of Cognitive Sciences, School of Social Sciences, University of California—Irvine, Irvine, CA 92717, U.S.A. [*Email* sperling@2.55.uci.edu].

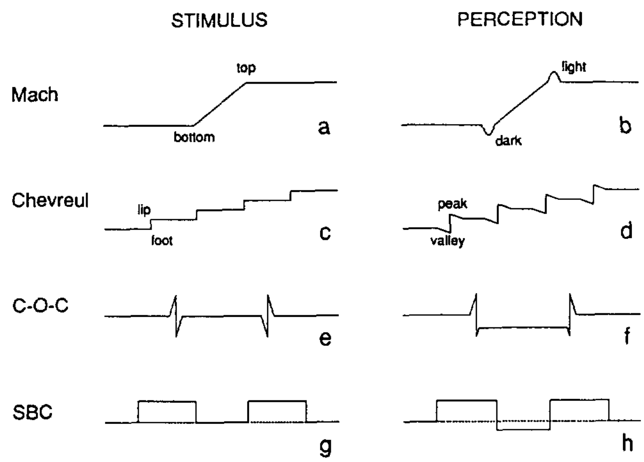

FIGURE 1. Schematic illustration of four spatial illusions: Mach bands, Chevreul staircase, Craik–O'Brien–Cornsweet, and Simultaneous Brightness Contrast. (a) Luminance modulation function (luminance as a function of space) for a classical Mach band stimulus. (b) The perceived brightness of (a). The relative minimum at the bottom and the relative maximum at the top are, respectively, the illusory dark and light Mach bands. (c) Chevreul staircase modulator. (d) An illusory valley is perceived at the foot of each step and an illusory peak at the lip of the step. (e) Luminance modulation function of a Craik–O'Brien–Cornsweet stimulus. (f) The illusion is the decrease in apparent brightness of the entire central region. (g) Luminance modulation function for the Simultaneous Brightness Contrast illusion. (h) The illusion is a decrease in apparent brightness of the entire central area.

the theory for second-order processing involves two successive stages: first, a stage of rectification (a grossly nonlinear transformation) and second, an analysis similar to the analysis of luminance stimuli. Here, in *fullwave* random textures, we demonstrate three further illusions that are second-order analogs of first-order luminance illusions.

Carriers and modulators

The root of our second-order illusions is a random texture, the carrier, in which the luminance $l(x,y)$ of each pixel x,y is chosen randomly and independently, and in which the expected luminance value $l_0 = E[l(x,y)]$ of every pixel is the same. Imposed on this *carrier* texture there is a spatial modulation $f(x)$ of contrast [Fig. 2(d)]. The modulator of contrast $f(x)$ in second-order textures serves the same role as a modulator of luminance in classical (first-order) patterns. However, in the second-order stimuli, only contrast modulation varies across space, the expected luminance is the same everywhere.

Most visual phenomena in the study of texture perception are independent of absolute luminance level for an extremely wide range of luminances. Therefore, it is convenient to define stimuli, even luminance stimuli, in terms of their point contrast.* Specifically, let the point contrast $c(x,y)$ of a *carrier* pixel at the point (x,y) be $c(x,y) = [l(x,y) - l_0]/l_0$ where l_0 is the mean expected value of luminance in the display area. Let the contrast modulator function be $f(x)$. Then the point contrast $s(x,y)$ of the *second-order* texture stimulus is defined by

$$s(x,y) = \frac{[l(x,y) - l_0]}{l_0}[1 + f(x)] = c(x,y)[1 + f(x)]. \quad (1)$$

For a first-order texture, the carrier is simply $c(x,y) = 1$, and the stimulus is 1 + the modulator. For a second-order texture, the stimulus is the *carrier* × (1 + the modulator). For a second-order texture, the expected value of contrast of the carrier is zero, $E[c(x,y)] = 0$; it is the variance of $c(x,y)$ (the power) that defines texture strength. To construct an actual second-order stimulus with pixel luminances $l_s(x,y)$, $s(x,y)$ from equation (1) and the desired l_0 are recombined:

$$l_s(x,y) = l_0 s(x,y) + l_0. \quad (2)$$

Recovery of the modulator: rectification

To recover the modulator function from a first-order stimulus, we simply measure the luminance at each point x and subtract the mean luminance. To recover the modulator function from a second-order texture stimulus, it is necessary to *rectify* the contrast values of the stimulus. We consider here *fullwave* and *halfwave* rectification. By *fullwave* rectification, we mean a monotonically increasing function of the absolute value of contrast, typically $|s(x,y)|$ or $s^2(x,y)$ [Fig. 2(a)]. Except for random fluctuations, a random texture, as defined by equation (1), becomes equivalent to an ordinary luminance pattern upon fullwave absolute value rectification. Chubb and Sperling (1989a, b) use the term *second-order* perception to refer to the perception of modulator patterns that are defined as in equation (1) and which require rectification to become accessible to standard linear analyses [matched linear filter followed by energy detection, e.g. Sperling (1964)].

Fullwave vs halfwave rectification

In addition to demonstrating and measuring second-order illusions, the present study seeks to determine whether the second-order illusions depend on *fullwave* or *halfwave rectification*. To do this, we create 'fullwave' textures whose spatial modulator $f(x)$ is recoverable by fullwave or halfwave rectification and 'halfwave' textures whose spatial modulator $f(x)$ is recoverable only by halfwave rectification.

There are good reasons to investigate both kinds of rectification. Halfwave rectification dominates the early stages of visual processing: i.e. the ordinary center–surround receptive fields of the retina function like

*The term contrast has two meanings: the contrast value at a point and a statistical property of an entire display. When it is necessary to distinguish these meanings, we use the term 'point contrast' $c(x)$ to designate the contrast value at a point: $c(x) = [l(x) - l_0(x)]/l_0$ where $l(x)$ is the luminance at point x and l_0 is the mean luminance of the display. The unmodified term 'contrast' is reserved for its more common use as a statistical property of the entire display, typically the expected value of the absolute value of point contrast or, occasionally, the r.m.s. value of point contrast.

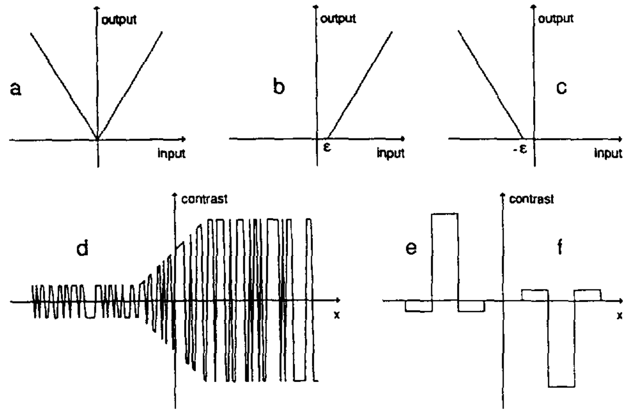

FIGURE 2. Rectifiers and their associated stimulus micropatterns. (a) The input–output characteristic of a fullwave rectifier. Any mirror-symmetric, U-shaped function would qualify, an absolute-value fullwave rectifier is illustrated. (b) Positive halfwave rectifier with a threshold, ε. (c) Negative halfwave rectifier with a threshold, $-\varepsilon$. (d) Cross-section of a binary noise carrier with a Mach band [Fig. 1(a)] modulation. (e) A plus-hat, a stimulus that in two dimensions has the same average luminance as the background. In the nine-pixel version, the surround is one-eighth height of center. (f) A minus-hat. The plus and minus hats, (e) and (f) respectively, produce nonzero outputs only in positive and negative halfwave rectifiers (b) and (c) respectively.

halfwave rectifiers. On-center cells (Kuffler, 1953) perform positive halfwave rectification, transmitting information primarily about increments in luminance in the centers of their receptive fields. Off-center cells transmit information primarily about decrements in luminance and are analogous to negative halfwave rectifiers. Ordinary vision ('what' we see) depends on both halfwave systems, on-center and off-center, and is represented by the difference between the two outputs: on-center minus off-center.

Current theories of visual processing (e.g. Sperling, 1989), and about illusions in particular (e.g. Burr & Morrone, 1994) concern both the contents of what is seen (e.g. whether a point appears to be light or dark) and the control of these contents by their neighborhood. Typically, the point-by-point contents appear as one term in an arithmetic expression and the control mechanisms appear as a multiplier or divisor term that represents shunting (vs subtractive) inhibition (Sperling & Sondhi, 1968). The question here, concerning illusions, is whether the control mechanisms that produce second-order illusions rely on halfwave or on fullwave rectification.

The ubiquity of halfwave rectification in early visual processing has tempted psychophysicists to propose halfwave theories of psychophysical functions (e.g. Watt & Morgan, 1985). In motion perception, however, fullwave rather halfwave processes seem to be dominant (Chubb *et al.*, 1989; Solomon & Sperling, 1994). Halfwave processes seem to be similarly silent in spatial interactions. A purely spatial interaction, the second-order version of the Simultaneous Brightness Contrast illusion [Fig. 1(g, h)] was shown to depend on fullwave, not halfwave interactions (Solomon *et al.*, 1993). Thus, an important question asked in present experiments is whether the interactions that result in second-order illusions occur in halfwave stimuli, or whether they are confined to fullwave stimuli. To understand such stimuli, we first need to define fullwave and halfwave rectification.

Rectifiers

Fullwave rectifier. For the present purposes, a fullwave rectifier is any monotonic increasing function of the absolute value of point contrast. In practice, fullwave rectification is usually assumed to be the absolute value or the square of point contrast (e.g. Wilson, Ferrera & Yo 1992), but it is not necessary here to be specific about the fullwave mechanism.

Halfwave rectifiers. Creating an effective halfwave texture (e.g. one that selectively stimulates only the on-system and not the off-system) requires an assumption about the halfwave mechanism. The assumption we make is that halfwave rectification, if it occurs, has a threshold. There is abundant evidence that near psychophysical thresholds, human vision has an approximately square law intensity characteristic (Nachmias & Sansbury, 1974; Stromeyer & Klein, 1974; Legge & Foley, 1980; Carlson & Klopfenstein, 1985), a so-called 'soft threshold'. If the human halfwave system had a hard threshold that was exactly matched to our halfwave stimuli, it would make our stimuli 100% selective in reaching only the appropriate system (e.g. positive halfwave stimuli to on-center system, negative to off-center) with zero crosstalk. However, less then perfect isolation is not critical for any of the observations or conclusions being made here (see Solomon & Sperling, 1994).

The halfwave rectification functions are illustrated in Fig. 2(b, c). Positive and negative halfwave rectification respectively, refer to functions $M^+(s)$ and $M^-(s)$ such that

$$M^+(s) = \begin{cases} 0 & s < \varepsilon \\ |s| - \varepsilon, & s \geqslant \varepsilon \end{cases} \quad M^-(s) = \begin{cases} 0 & s > -\varepsilon \\ |s| - \varepsilon, & s \leqslant -\varepsilon \end{cases}. \qquad (3)$$

In equations (3), ε represents a small positive constant, the threshold. To re-iterate: the complication of a threshold is not necessary in the definition of fullwave rectification (although soft thresholds undoubtedly do occur in perceptual fullwave processing), but ε is convenient in order to provide a simple analysis of the stimuli that are designed to stimulate halfwave processes.

Luminance, fullwave, and halfwave stimuli

Luminance and fullwave stimuli. We proceed to examine Mach bands, Chevreul and Craik–O'Brien–Cornsweet illusions in their original forms (luminance stimuli) or in second-order versions that either require fullwave or require halfwave transformations for extraction of the modulator function, $f(x)$. When the absolute value rectifier of Fig. 2(a) is applied to the fullwave stimulus of Fig. 2(d), it is quite obvious that the direct result is the ramp modulator itself.

Halfwave extraction of modulators in fullwave stimuli. Applying positive halfwave rectification to the ramp of

Fig. 2(d) would extract the modulator of the upper half of the signal, the negative halfwave rectifier would extract the modulator of the bottom half of the signal, and give a complementary result. That is, the locations where the signal is positive are the compliment of the locations where it is negative. In our dynamic stimuli, however, a new random instantiation is produced every 67 msec (15 new frames per sec) so that positive and negative halfwave outputs would follow rapidly upon each other at each location. Thereby, over time, the expected output is exactly the same for the negative and positive halfwave rectifiers at each location.

Bases of halfwave action. We consider three possibilities for the action of halfwave rectifiers in the control of spatial illusions. *(1) Outputs of halfwave rectifiers add.* This is exactly equivalent to fullwave rectification; it is not a different computation. *(2) Outputs of halfwave rectifiers subtract.* This would be the normal mode of vision: whites appear white, blacks appear black. But is it the operative transformation in the formation of spatial illusions? In the fullwave stimuli, the expected positive and negative halfwave output is the same everywhere. Therefore, if the positive and negative halfwave outputs were subtracted, and if there were any spatial or temporal averaging—the normal mode for control mechanisms—then there would be complete cancellation of halfwave outputs. It follows that, if halfwave rectification followed by subtraction were critical in creating illusions, the fullwave stimuli would not show any illusions. (But they do.) *(3) There is a separate analysis by each halfwave system.* That is, a stimulus is analyzed either by (a) the on-center cells acting alone without any interaction by off-center cells, or by (b) the off-center cells, acting alone; or by both (a) and (b). This is the mode of action that is usually assumed when halfwave interactions are under discussion (e.g. Watt & Morgan, 1985). In this case, the modulation would be extracted from fullwave stimuli by each halfwave process.

Halfwave stimuli. To differentiate between fullwave processes and isolated halfwave processes, we create halfwave stimuli in which separately acting positive and negative halfwave processes, if they existed, each could create an illusion. These stimuli use the 'Mexican hat' micropatterns (see the *Method* section of Expt 1 for a definition) as the carrier, but vary the local probability of a + or − hat rather than, as in the fullwave stimulus, the modulation amplitude of the hat. Because the absolute value of the amplitude distribution is the same everywhere in the stimulus, fullwave processes see a completely uniform stimulus and, obviously, cannot be the basis of an illusion.

Calibration. Fullwave and halfwave stimuli are easily calibrated photometrically and psychophysically so that the modulator is invisible to first-order process. The calibration of halfwave stimuli so that they are invisible to fullwave mechanisms is described by Solomon and Sperling (1994). Beyond the calibration procedures, the nature of the results will indicate that partial misdirection of any of the stimuli into an unintended system is of no consequence.

GENERAL METHOD

The displays for the experiments were presented on a photometrically calibrated computer-driven CRT with a white screen.* New frames were generated every 16.7 msec (60 Hz). The mean display luminance was 44.1 cd/m^2; the contrast range was $\pm$ 0.934; there were 256 gray levels with equal linear spacing.

All the subsequent contrast values refer to proportions of this maximum contrast. Every random pattern was displayed for four successive frames (66.7 msec). Then, to eliminate any figural cues and to render negligible any effects of statistical fluctuation in generating the stimulus, a new independent realization of the random carrier texture was displayed. Thus, the rate of new patterns was 15 Hz.

EXPERIMENT 1: CLASSICAL AND SECOND-ORDER MACH BANDS

Method

A texture is called a 'Mach band pattern' if its contrast modulator $f(x)$ can be described as a ramp function of horizontal spatial variable x [Fig. 1(a)]. We generated three second-order Mach bands (two fullwave, one halfwave) and one first-order (luminance) Mach band. The patterns all have the same overall spatial dimensions: 6.47 × 0.97 deg (600 × 90 pixels) embedded in a screen of 8.63 × 4.85 deg, luminance of 44 cd/m^2, viewed at 110 cm. There is wide latitude in the stimulus dimensions for these illusions (Fiorentini & Radici, 1958; McCollough, 1955; Hartwig, 1958; Ercoles & Fiorentini, 1959). The dimensions were chosen to concurrently maximize the first- and second-order illusions within the constraints of the apparatus. The Mach band modulator is

$$f(x) = \begin{cases} c_1 & x < -a \\ \dfrac{c_2 + c_1}{2} + \dfrac{x(c_2 - c_1)}{2a} & -a \leqslant x \leqslant a \\ c_2 & x > a. \end{cases} \quad (4)$$

The ramp occupies the central $2a$ deg (from $\pm a$ deg), and ranges from a contrast of c_1 to c_2. In all our Mach bands, $2a = 0.86$ deg.

*The displays for the experiments were presented on a Leading Technologies 1230V (12 in. diagonal) monochrome graphics monitor, using an ATVista image display system controlled by an IBM 486PC compatible computer. The dials on the monitor were set to maximum brightness and medium contrast (a preset notch in the dial). With this setting, the luminance of the monitor was 2.9 cd/m^2 when every pixel was given the lowest gray level and 85.3 cd/m^2 when every pixel was given the greatest gray level. A lookup table had been generated with a psychophysical procedure which linearly divides the whole luminance range to 256 gray levels. We chose the background luminance to be that value which, when it is assumed by every pixel, produces 0.5 × (85.3 + 2.9) = 44.1 cd/m^2. The maximum obtainable pixel contrast for any stimulus point is thus (85.3 − 44.1)/44.1 = 0.934.

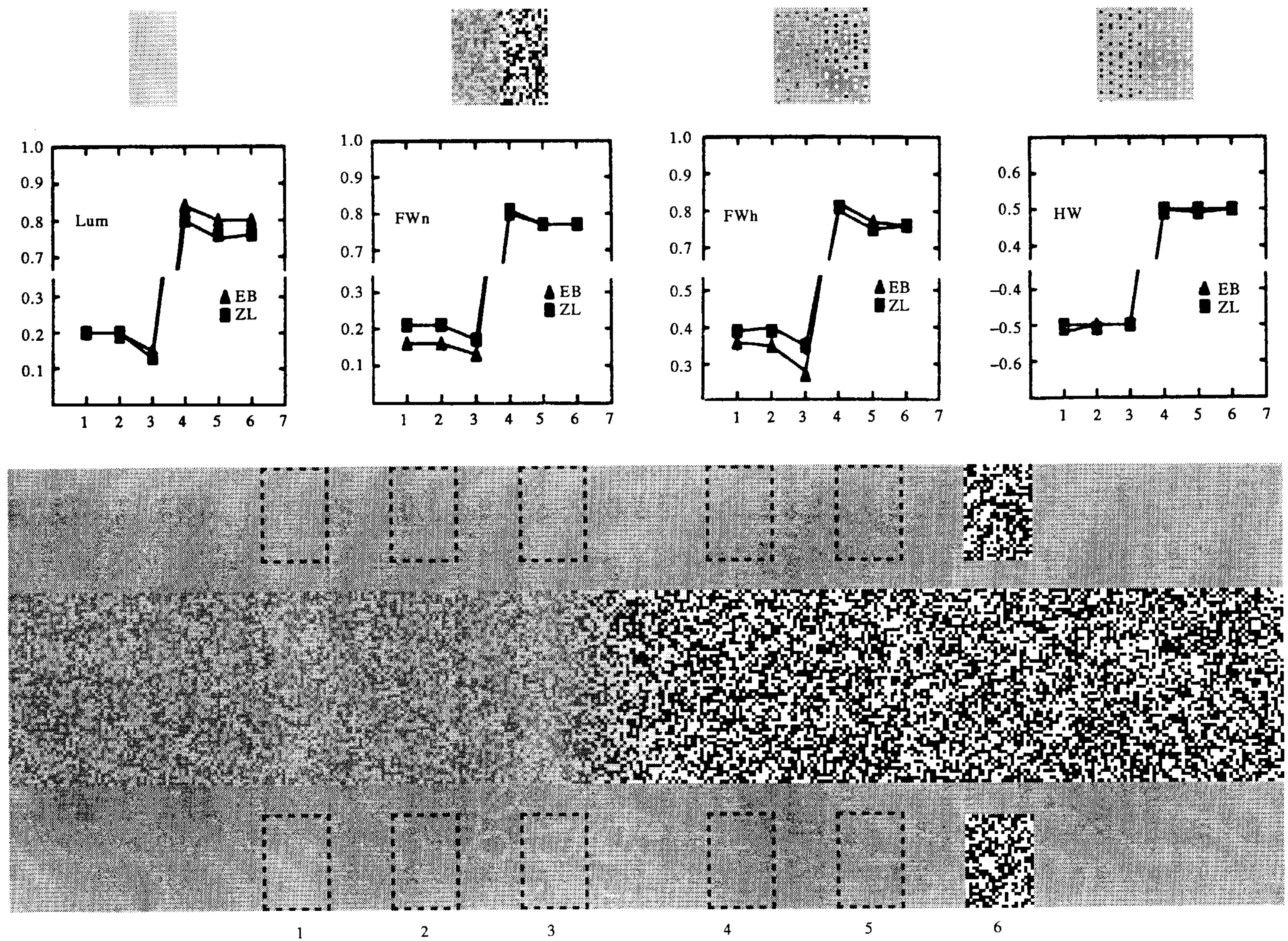

FIGURE 3. Mach band stimulus patterns and the magnitudes of their perception. The top row shows samples of the carrier texture. The middle row shows the matched contrast for four different kinds of Mach band patterns. The lower row depicts a fullwave-noise Mach band pattern along with two measurement bars at location '6'; the other locations are schematically indicated. In the middle row the abscissas indicates the location of the measurement bars designated as 1–6 from left to right. For luminance stimuli, the ordinate is the matching contrast; for the fullwave stimuli, the ordinate is the the absolute value of the contrast modulation. Lum, luminance; FWn, fullwave-noise; FWh, fullwave Mexican hats; HW, halfwave. △ and □ indicate observers EB and ZL respectively. For optimum effect, try different viewing distances.

Fullwave random-pixel Mach pattern (FWn). The first fullwave Mach band pattern is a random texture in which the contrast of each carrier pixel is chosen randomly and independently to be either ± 1 [Fig. 2(d)]. The modulator is the Mach band modulator described by equation (4) with left plateau contrast $c_1 = 0.20$ and right plateau contrast $c_2 = 0.80$. The carrier/modulator combination is described by equation (1); the stimulus is shown in Fig. 3.

Fullwave Mexican-hat Mach pattern (FWh). The carrier texture of the second fullwave Mach band pattern is composed of center–surround micropatterns (Carlson, Anderson & Moeller, 1980) called 'Mexican hats'. Each Mexican hat consists of a central 2×2 pixel square randomly embedded in a 6×6 pixel square. The contrasts of the central 4 and surrounding 32 pixels are carefully balanced so that the average contrast of a whole Mexican hat is zero [Fig. 2(e,f)]. In the carrier, the hat centers are chosen randomly to be either light (center contrast = + 1) or dark (center contrast = − 1) with equal probability. The Mach band modulator is described by equation (4) with left plateau contrast $c_1 = 0.40$ and right-plateau contrast $c_2 = 0.80$. (The contrast of $c_1 = 0.40$ was used because hats micropatterns with contrasts of 0.2, analogous to the full c_1 contrast, were not clearly visible.)

Halfwave Mexican-hat Mach pattern (HW). The carrier texture for the halfwave Mach band pattern is composed of Mexican hats with center contrasts of 0.50 (center-light) or −0.50 (center-dark) [Fig. 2(e,f)]. The modulator $f(x)$ describes the *proportion* of center-light hats: $f(x) = 0$ indicates 0% light-center hats (100% dark-center hats), $f(x) = 1$ indicates 100% light-center hats. Interpreting the Mach band modulator $f(x)$ in equation (4) as the probability of light hats, yields $c_1 = 0$ and $c_2 = 1.0$ as in the fullwave Mach bands.

Luminance Mach bands (Lum). In the control condition, an original, luminance Mach band pattern, was made with carrier $c(x,y) = 1$, and the modulator $f(x)$ varying from $c_1 = 0.2$ to $c_2 = 0.8$ [$s(x,y)$ varies from 1.20 to 1.80 times the background luminance level].

Estimating perceived magnitude of Mach bands. The perceived magnitude of the Mach bands was quantified by means of a matching procedure (Lowry & DePalma, 1961) in which a slice of the Mach band stimulus was compared to a pair of adjacent bars that were composed of a similar texture (Fig. 3). On each trial, a Mach band stimulus plus two adjacent bars was presented until the observer made his judgment (usually within 1 or 2 sec). The observer's task was to judge whether the contrast of the bars was greater or smaller than the contrast of the co-linear vertical slice of the Mach band stimulus.

From trial-to-trial, the contrast of the bars was varied by means of an interleaved staircase procedure (Levitt, 1971). Pairs of measurement bars were tested at six experimenter-defined locations with each Mach pattern. On each trial, a randomly chosen pair of the measurement bars was presented. Subjects were instructed to fixate the midpoint between the bars, and to make a contrast comparison between the fixation point and the measurement bars. The staircase procedure used two interleaved sets of trials—one converging to $X_{29.3}$, and another converging to $X_{70.7}$. At least eight runs were collected for each bar position, and the last six runs were used to estimate $X_{29.3}$ and $X_{70.7}$. The matching level was taken as the mean of $X_{29.3}$ and $X_{70.7}$. When the psychometric function is a Normal distribution function, the estimate σ of its standard deviation is $(X_{70.7} - X_{29.3})/1.09$.

For each subject and each pair of measurement bars, two separate sets of eight or more staircases were run and the results were averaged. Two subjects participated in the measurements; five other observers viewed the displays and reported their perceptions.

Results

When viewing the fullwave Mach band patterns (FWn and FWh) without the measurement bars, all seven observers reported that they perceived a low contrast band near the low-contrast end of the ramp and a high contrast band near the high-contrast end of the ramp.

TABLE 1. The percentage magnitude of perceived Mach bands in first- and second-order stimuli

		ZL			EB			
Carrier	Band	Magnitude	SE	σ	Magnitude	SE	σ	Mean magnitude
First order								
Lum	Dark	7.5	0.76	2.0	4.2	0.66	1.2	5.9
	Light	4.6	1.2	3.8	3.9	0.83	3.9	4.3
	Mean	6.6	0.98	2.9	4.2	0.75	2.6	5.0
Second order								
FWn	Dark	3.7	1.3	2.8	3.5	0.65	2.3	3.6
	Light	3.7	1.2	3.1	2.7	1.1	3.4	3.2
	Mean	3.7	1.2	2.9	3.1	0.88	2.8	3.4
FWh	Dark	3.8	1.7	3.0	8.2	1.8	2.7	6.0
	Light	5.1	1.0	4.6	4.5	0.87	4.5	4.8
	Mean	4.5	1.4	3.8	6.4	1.3	3.6	5.4
HW	Dark	0.32	0.91	3.0	0.08	0.75	3.1	0.20
	Light	0.71	0.86	3.3	0.57	0.67	3.1	0.64
	Mean	0.52	0.89	3.2	0.33	0.71	3.1	0.42

Lum, luminance Mach bands; FWn, fullwave noise Mach bands; FWh, fullwave hats Mach bands; HW, halfwave hats bands; SE, standard error of band magnitudes; σ, standard deviation of the psychometric function which gives the probability as a function of bar contrast of judging an adjacent bar as having more contrast than the test area.

These subjective impressions were quite strong. However, no observer was confident that he or she saw any visible bands in the halfwave stimulus.

The contrast-matching judgments with the reference bars confirmed and quantified the general subjective impressions, as shown in Fig. 3 and Table 1. The second row of Fig. 3 shows the actual matched contrasts for each subject and stimulus. The magnitude of the perceptual Mach bands is estimated by the magnitude of the local minima and maxima in matched contrast near the ramp boundaries. These measured minima and maxima were similar for the luminance stimulus and for the two fullwave textures.

All the differences between contrasts at Mach bands and matched contrast at the neighboring points are statistically significant at 0.005 level for the fullwave and the luminance stimuli. None of the differences is significant for the halfwave stimuli. Table 1 gives the estimated heights and depths of the illusory Mach bands—the difference between the judged contrast at the maximum or minimum and the mean contrast of adjacent plateau points. The last column of Table 1 shows the mean sizes of bands for each type of stimulus averaged over positive and negative bands and over subjects. (Note that the units in Table 1 are %; the units of Fig. 3 are fractions.) Relative to the magnitude of luminance bands (5.0%), the fullwave hats bands are slightly larger (5.4%) and the fullwave noise bands are somewhat smaller (3.4%).

Table 1 also gives the standard error of the estimates of band magnitudes. σ in Table 1 is the standard deviation of the psychometric function which gives the probability of judging an adjacent bar as having more contrast than the test area as a function of bar contrast. There are no bands and no significant deviations from flatness in the plateaus of the halfwave stimulus. In summary, we measured Mach bands of generally similar magnitudes in luminance and in fullwave-contrast stimuli, but found no bands in halfwave stimuli.

EXPERIMENT 2: LUMINANCE AND CONTRAST CHEVREUL ILLUSIONS

Method

The Chevreul illusion can be demonstrated using a contrast modulator $f(x)$ which is made of monotonically increasing (or decreasing) steps. We generated one first-order (luminance) and two second-order (one fullwave and one halfwave) Chevreul stimuli. Each stimulus has five steps and all stimuli have the same overall spatial dimensions: 14.25×8.59 deg (400×240 pixels) embedded in a screen of 26.38×16.89 deg at a viewing distance of 81.3 cm. The multi-step modulator is

$$f(x) = \begin{cases} c_1 & x < a \\ c_1 + \Delta c & a \leqslant x < 2a \\ c_1 + 2\Delta c & 2a \leqslant x < 3a \\ c_1 + 3\Delta c & 3a \leqslant x < 4a \\ c_1 + 4\Delta c & x \geqslant 5a. \end{cases} \quad (5)$$

The spatial extent a of each step is 2.87 deg.

Fullwave random-pixel Chevreul pattern (FWn). The fullwave Chevreul pattern is a random texture in which the contrast of each carrier pixel is chosen randomly and independently to be either ± 1; the modulator is the Chevreul modulator described by equation (5) with contrast $c_1 = 0.10$ and step size $\Delta c = 0.20$. The carrier/modulator combination is described by equation (1); the stimulus is shown in Fig. 4 (right panels).

Halfwave Mexican-hat Chevreul pattern (HW). The carrier texture for the halfwave Chevreul pattern is composed of Mexican hats with center contrasts of 0.50 (center-light) or -0.50 (center-dark) [Fig. 2(e,f)]. The modulator $f(x)$ describes the *proportion* of center-light hats: $f(x) = 0$ indicates 0% light-center hats (100% dark-center hats), $f(x) = 1$ indicates 100% light-center hats. If we interpret the Chevreul modulator $f(x)$ in equation (5) as describing the probability of center-light hats, then we have $c_1 = 0$ and step size $\Delta c = 0.20$.

Luminance Chevreul pattern (Lum). The first-order (luminance) Chevreul pattern is defined by equation (1) with a constant luminance carrier $c(x,y) = 1$, and a modulator [$f(x)$, equation (5)] beginning with $c_1 = -0.16$ and continuing in steps of $\Delta c = 0.08$; thereby, $s(x)$ [equation (1)] varies from 0.84 to 1.16 times the background luminance level (Fig. 4, left panels).

Estimating perceived magnitude of Chevreul illusions. The perceived magnitude of the Chevreul illusions was quantified by means of a nulling procedure in which subject increases or decreases the contrast of a hill that is added to a foot or a valley that is added to a lip of a step until the perceived step appears to be flat. In this manner, the illusory Chevreul bands disappear. While adding incremental hills and valleys, the rest of $f(x)$ was kept unchanged. The contrast change produced by an incremental hill or valley in the neighborhood of the edge is described by an exponential decaying function. That is, the contrast increment or decrement $g(y)$ diminishes as a function of y, the distance from the edge:

$$g(y) = A\mathrm{e}^{-y/\lambda}, \quad y < a/2 \quad \text{otherwise } g(y) = 0. \quad (5a)$$

In equation (5a), A is the amplitude of the change (positive for hills, negative for valleys), and λ is a spatial constant which was fixed at $a/4$ (0.72 deg) on the basis of pilot studies.

An interleaved staircase procedure (Levitt, 1971) was used to measure the amplitude A. Because A is the amplitude added to cancel the illusory band, $-A$ is taken as the amplitude of the illusory band. On each trial, a Chevreul stimulus plus two pairs of adjacent bars were presented for 2 sec. One pair of the bars was above and below a given edge indicating the step edge that was being changed. Another pair of bars was above and below the middle of a step. The task of the observer was to judge whether the contrast of the edge was greater or smaller than the contrast of the center of the step.

The staircase procedure used two interleaved sets of trials—one converging to $X_{29.3}$, and another converging to $X_{70.7}$. At least 10 runs were collected for each trial, and

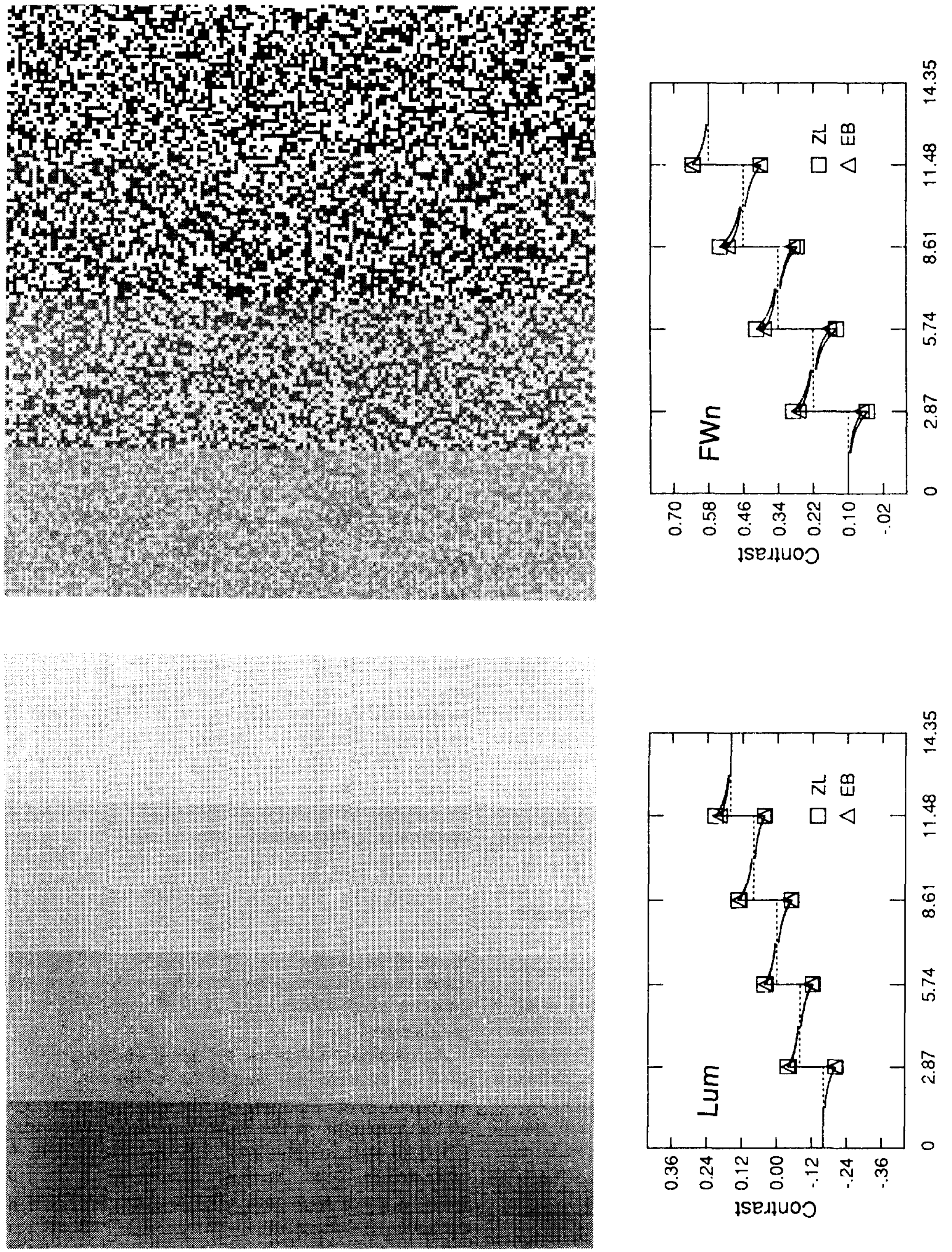

FIGURE 4. *Caption on facing page.*

TABLE 2. The percentage magnitude of a stimulus contrast required to cancel first- and second-order Chevreul illusory peaks and valleys

Carrier		Band	ZL Magnitude	ZL SE	ZL σ	EB Magnitude	EB SE	EB σ	Mean magnitude
First order									
Lum	1	Foot	+4.2	0.79	1.8	+4.1	0.90	1.3	+4.2
		Lip	−4.2	0.97	2.1	−3.6	0.70	0.64	−3.9
	2	Foot	+4.3	0.97	0.76	+3.8	0.72	1.3	+4.1
		Lip	−4.2	0.84	0.51	−3.7	0.72	1.4	−4.0
	3	Foot	+5.1	0.84	0.94	+4.9	0.85	1.2	+5.0
		Lip	−5.2	0.76	0.39	−4.8	0.59	1.7	−5.0
	4	Foot	+3.8	0.69	0.61	+3.5	0.91	0.65	+3.7
	5	Lip	−5.1	0.47	0.61	−3.6	0.60	0.92	−4.3
		Mean (abs)	4.5	0.79	0.97	4.0	0.75	1.1	4.3
Second order									
FWn	1	Foot	+6.4	0.58	2.0	+4.5	0.78	1.3	+5.4
		Lip	−7.0	0.79	0.15	−5.1	0.72	1.1	−6.1
	2	Foot	+8.0	1.4	1.5	+5.7	0.84	2.1	+6.8
		Lip	−7.5	1.3	1.4	−4.8	0.77	1.4	−6.2
	3	Foot	+6.5	1.3	0.91	+5.1	0.64	1.7	+5.8
		Lip	−8.2	1.2	1.3	−5.2	0.72	1.5	−6.7
	4	Foot	+5.8	0.60	1.7	+5.8	0.72	2.6	+5.8
	5	Lip	−5.5	0.98	2.5	−5.3	0.94	1.7	−5.4
		Mean (abs)	6.9	1.0	1.4	5.2	0.77	1.7	6.0

Lum, luminance Chevreul illusion; FWn, fullwave Chevreul illusion; +indicates added contrast at foot to cancel a valley; −indicates subtracted contrast at lip to cancel a peak; SE, standard error of the illusion magnitudes; σ, standard deviation of the psychometric function which gives the probability as a function of added or subtracted contrast of judging a valley or a peak as having more contrast than the center of the same step. The number under column 'Band' is the step number.

the last eight runs were used to estimate $X_{29.3}$ and $X_{70.7}$. The matching level was taken as the mean of $X_{29.3}$ and $X_{70.7}$.

Two subjects participated in the measurements; four other observers viewed the displays and reported their perceptions.

Results

When viewing the fullwave noise (FWn) and luminance Chevreul (Lum) patterns, all six observers reported that they perceived low contrast bands on the foot side of edges and high contrast bands on the lip side of edges [Fig. 1(d)]. These subjective impressions were quite strong. However, none of our subjects could perceive any illusive bands when they were shown the halfwave Chevreul pattern. We restricted the measurement procedure to the fullwave and luminance steps.

The nulling procedure confirmed and quantified the general subjective impressions, as shown in Fig. 4 and Table 2. The lower panels in Fig. 4 shows the actual matched contrasts for each subject and stimulus, and represents the appearance of the illusory bands. To reiterate, the magnitude of the illusory Chevreul bands is estimated by the magnitude of the incremental hills and valleys [equation (5a)] needed to cancel the illusion. As Fig. 4 illustrates, the measured amplitudes were quite similar for the first-order luminance stimulus and for the fullwave noise texture.

Table 2 gives the estimated heights and depths of the Chevreul illusions—the magnitude of A at every foot and lip. The last column of Table 2 shows the mean sizes of bands for each type of stimulus averaged over all the bands and over subjects. (Note that the units in Table 2 are %; the units of Fig. 4 are fractions.) The magnitude of luminance bands is 4.3%, which is 54% of the step size (8.0%). The magnitude of the fullwave noise bands is 6.0%, which is 50% of the step size (12%).

Table 2 also gives the standard error of the estimates of band magnitudes. σ in Table 2 is the standard deviation of the psychometric function which gives the probability as a function of added or subtracted contrast in judging an edge as having more contrast than the center of the same step. In summary, measurement of the Chevreul illusion show that it is extraordinarily large, and of generally similar magnitude in first-order luminance and in second-

FIGURE 4. *(opposite)* Chevreul stimulus patterns and the magnitudes of peaks and valleys inferred from illusion-cancelling decrements and increments. The top panels shows the two different kinds of Chevreul patterns. The number of steps illustrated is four (the experiments used five) and the contrasts are exaggerated to compensate for the reproduction process. The bottom-left panel shows the inferred perceived luminance, the bottom-right panel shows the inferred perceived contrast. There are individual measurements for each step and subject. The abscissas indicate spatial location. The ordinates are the step heights minus the illusion-cancelling contrast increments and decrements. Lum, luminance; FWn, fullwave-noise. □ and △ indicate observers ZL and EB respectively. The steps are numbered 1, 2, ..., 5 from the left (Table 2).

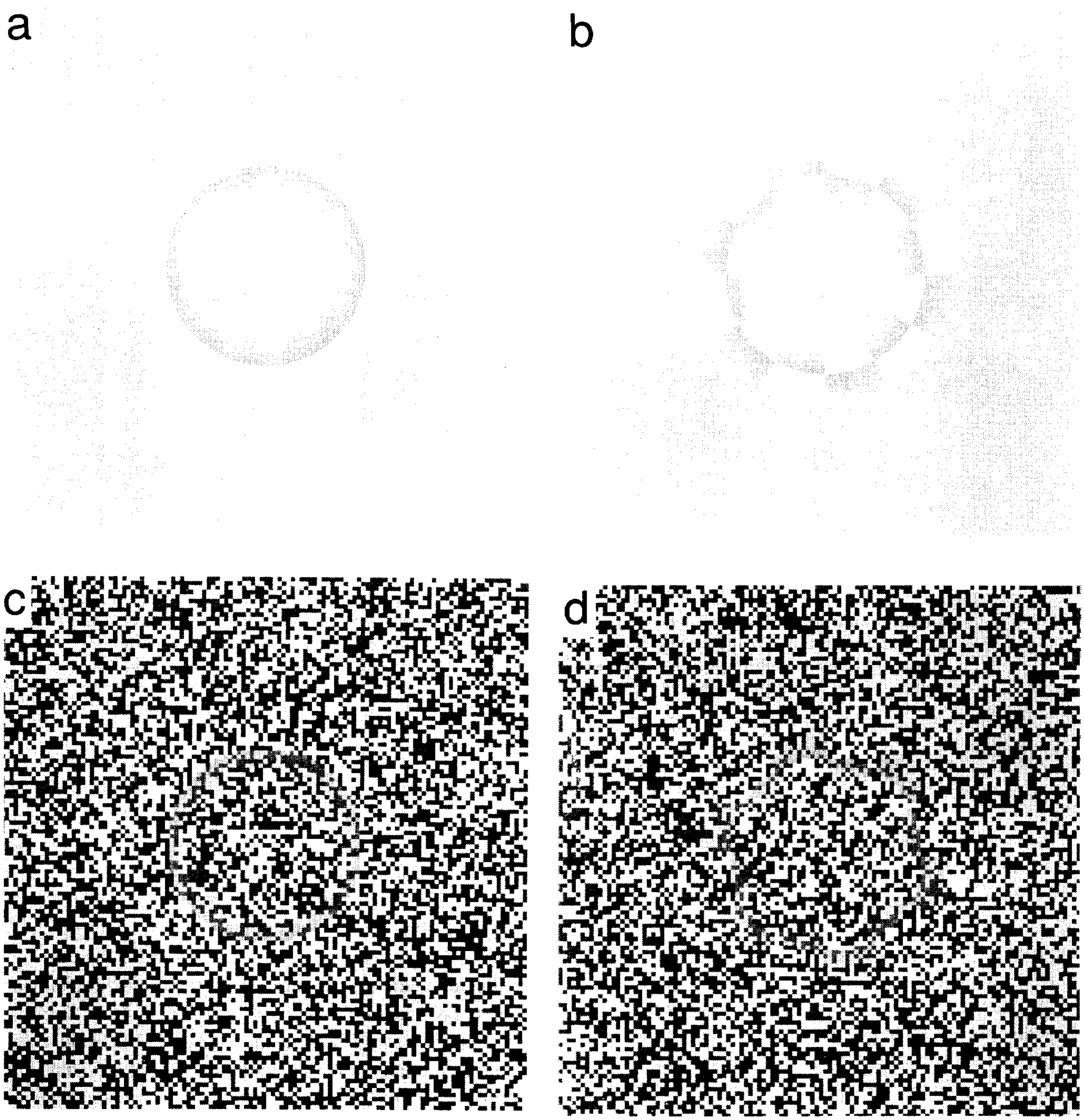

FIGURE 5. Luminance and fullwave-noise Craik–O'Brien–Cornsweet illusion (a,c) and comparison patterns (b,d). Contrasts are exaggerated to compensate for the reproduction process. The center of each comparison pattern has the same physical contrast as the center of the corresponding illusion pattern. Any perceived difference between the centers of (a) and (b) or (c) and (d) would indicate a Craik–O'Brien–Cornsweet illusion.

order fullwave-contrast stimuli. No illusory bands occurred in halfwave stimuli.

EXPERIMENT 3: CRAIK–O'BRIEN–CORNSWEET ILLUSION

Method

Experimental stimuli. The method is to create radially symmetric stimuli that exhibit the Craik–O'Brien–Cornsweet (C–O–C) illusion, and to match the magnitude of perceived brightness at the center of these stimuli to the perceived brightness at the center of comparison stimuli. The C–O–C stimuli are composed of textures whose modulator $f(r)$ is a function only of radius r in a polar coordinate system. The modulator $f(r)$ consists of four segments: (1) a constant inner disk; (2) an inner ring with smaller than average values of the modulator; (3) an adjacent, concentric outer ring with larger values; (4) and the background with the same value as the inner disk (see Figs 1 and 5):

$$f(r) = \begin{cases} c_0 & r \leqslant 2.86 \text{ deg} \\ c_0(1 - m\exp[-\lambda(4.63 - r)]) & 2.86 \leqslant r < 4.63 \text{ deg} \\ c_0(1 + m\exp[-\lambda(r - 4.63)]) & 4.63 < r \leqslant 6.02 \text{ deg} \\ c_0 & 6.02 < r. \end{cases} \tag{6}$$

The carrier texture for the fullwave C–O–C pattern is the random noise texture in which the contrast of each pixel of the carrier is chosen randomly and independently to be either +1 or -1. The modulator is defined by equation (6) with $\lambda = 1.0/1.77\,\text{deg}^{-1}$, $m = 0.43$ and $c_0 = 0.70$ [Fig. 5(b)].

The carrier texture for halfwave Mexican-hat C–O–C pattern is composed of Mexican hats with center contrasts of 0.50 (center-light) or -0.50 (center-dark) [Fig. 2(e,f)]. As above, the halfwave modulator $f\,(r)$ describes the *proportion* of center-light hats: $f(r) = 0$ indicates 0% light-center hats (100% dark-center hats), $f(r) = 1$ indicates 100% light-center hats. Interpret the C–O–C modulator $f(r)$ in equation (6) as describing the probability of light hats yields $\lambda = 1.0/1.77\,\text{deg}^{-1}$, $m = 0.43$ and $c_0 = 0.5$.

In the first-order (luminance) stimuli, the carrier was replaced with a uniform field of intensity 1.0, and the same modulator as for the fullwave stimulus was used [Fig. 5(a)].

Comparison stimuli. Comparison patterns are made by multiplying the modulator of equation (6) by a function $g(\theta)$ of angle θ that changes the sign of the modulation every 60 deg [see Fig. 5(b,d)]. Since the direction of the induced C–O–C effect is changed every 60 deg, the average effect is expected to be zero. Therefore, to make possible a match to the perceived contrast of the C–O–C stimuli, the actual contrast of the center of the comparison stimulus has to be absolutely raised or lowered. Thereby, we compare the test stimulus (with the C–O–C illusion) to a comparison stimulus that looks generally similar but has a real physical contrast reduction instead of an induced illusory contrast reduction.

Seven comparison patterns, differing only in inner disk contrast values, were displayed simultaneously with the C–O–C patterns. Subjects were instructed first to look at the C–O–C pattern for 5 sec and then to find and select the comparison stimulus whose inner disk contrast best matched the center contrast of the C–O–C pattern. The values of the test contrast was 0.7; based of pilot studies, values of comparison contrasts were chosen from 0.58 to 0.70 in steps of 0.02.

The precision of contrast comparisons was estimated by taking as the test stimulus not the C–O–C pattern but one of the comparison patterns and requiring the subjects to select the nearest match from the set of comparisons patterns that, in fact, included an exact match.

Subjects. The first author and four observers from among graduate students who had no prior familiarity with the C–O–C illusion served as subjects.

Results

All subjects, indeed for everyone who has seen the fullwave C–O–C pattern, has invariably matched it to a comparison pattern with lower center contrast. The C–O–C stimulus reliably produces an illusory reduction of contrast. For the five subjects, the C–O–C stimulus with a center of contrast 0.70 was matched, on the average, to comparison centers with contrast 0.64, the range being 0.62–0.66. The precision in all the judgments is estimated to be 0.012. On the average, there is a $7 \pm 1\%$ contrast reduction attributable to the second-order C–O–C illusion.

The five subjects could barely make out the 'rings' in the halfwave C–O–C pattern; they did not perceive any change in the interior of the disk relative to the exterior or to a comparison disk. Halfwave stimuli yielded no illusion to measure.

For the first-order luminance C–O–C pattern (0.70 contrast), the average matching contrast was 0.62 with a precision of 0.016. For these stimuli, there was a tendency for the first-order luminance C–O–C illusion to be slightly stronger than the second-order texture illusion. As it happens, the difference in the size of the C–O–C illusion between 0.62 (for the first-order pattern) and 0.64 (for the second-order pattern) was not statistically significant. We conclude that a fullwave texture stimulus and a luminance stimulus exhibit Craik–O'Brien–Cornsweet illusions of similar magnitudes for the stimuli investigated here. No Craik–O'Brien–Cornsweet illusion was observed with halfwave stimuli.

DISCUSSION

Fullwave vs halfwave rectification in second-order illusions

Fullwave rectification treats light spots and dark spots equivalently. Since humans can discriminate quite well between white and black, fullwave rectification is not a candidate mechanisms for ordinary vision. It is relevant to illusions because it would be an appropriate mechanism for gain-control mechanisms that modulate vision.

The modulator can be extracted from the fullwave stimuli by either fullwave or halfwave rectification (see section Luminance, fullwave, and halfwave stimuli). The modulator can be extracted from halfwave stimuli by halfwave rectification but not fullwave rectification. Since illusions occurred with fullwave stimuli, and not with halfwave stimuli, it seems plausible that fullwave rectification is responsible for the illusory component in the perception of the stimuli studied here. We consider a few factors in more detail.

Both fullwave-hat and halfwave stimuli use identical Mexican-hat microelements. The critical difference is that, in fullwave stimuli, the amplitude of both plus hats and minus hats is modulated, in halfwave stimuli the sign of the hat (plus or minus) is modulated. Indeed, the signal strength for a halfwave modulator is much stronger in the halfwave stimuli than fullwave stimuli. The fullwave modulation was only between 40% and 80%; in the halfwave stimuli, the modulation was the maximum possible: from 100% to 0% for the plus hats and for the minus hats.

In the case of Mach band modulators, the halfwave stimuli were easily perceived, correctly, to contain areas of white and dark dots that ramp into each other. The subjects failed to perceive an illusory enhancement of these perceived ramps—the Mach bands. This failure to contain an illusion was documented in more detail (but not in any fundamentally different way) by the matching procedure. In the case of the other illusions (Chevreul, C–O–C), the halfwave stimuli also failed to produce the illusory percept for any subject. It did not seem worthwhile to further document the zero magnitude of these nonillusions.

The Mach band, Chevreul, C–O–C modulators all produced their characteristic illusions when implemented as fullwave stimuli and showed no illusions as halfwave stimuli. The conclusion seems inescapable that the process responsible for the illusory component in the perception of these stimuli depends on fullwave rectification. These results can be viewed as experimental evidence for the plausibility of the energy computations proposed to account for these illusions (see Burr & Morrone, 1994, for a review). 'Energy' is an instance of square-law fullwave rectification.

It would have been desirable to have a fullwave stimulus whose modulator was inaccessible to halfwave rectification, but none such occurred to us. In the case of second-order motion perception, there is such a stimulus. As in these spatial illusions, second-order motion perception seems to depend on fullwave, not halfwave, rectification (Lu & Sperling, 1995), although some subjects have a very attenuated ability to perceive halfwave motion (Solomon *et al.*, 1994). However, all subjects easily perceive unambiguous motion in a stimulus that is unambiguous after fullwave rectification but ambiguous after halfwave rectification (Chubb & Sperling, 1989a,b). Where a positive test, rather than a test by elimination, was possible, it confirmed the conclusions arrived at by the elimination procedure.

The printed appearance of second-order illusions

Printed versions of second-order Mach, Chevreul, and C–O–C illusions are less striking than printed versions of the corresponding first-order illusions, although the opposite is true for the Simultaneous Brightness Contrast illusion. We consider four factors.

(1) Static vs dynamic stimuli. The illusory stimuli that were measured in this study were dynamic; printed versions are static. In our preliminary measurements, the change from dynamic to static mode decreased the magnitude of the (second-order) illusion to 75–80% of the first-order magnitude.

(2) Printed vs CRT image. Although there is an obvious loss in quality of the printed illusion, it is difficult to quantify. The second-order Mexican hat textures were not illustrated because they do not print sufficiently well (e.g. Solomon & Sperling, 1994, Figs 2 and 3, pp. 2243–2244). Based on the page proofs of this paper, we estimate the loss of contrast in the printed fullwave-noise stimulus (Fig. 3) to be insignificant.

(3) Discriminability of intensity changes vs contrast changes. The ability to discriminate intensity and contrast changes is measured in the Chevreul illusion by the σ (Table 2) of the cancelling increments and decrements. (σ is the standard deviation of a staircase estimate, not of individual judgments.) It measures the ability of subjects to discriminate intensity and contrast changes at the point of the illusion. For the first-order peaks and valleys, the mean σ is 1.04%; for the second-order it is 1.55%. Contrast discriminability is two-thirds of luminance discriminability. Even if the first- and second-order illusions were of the same percentage magnitude, the second-order illusion would be only two-thirds as many jnds above threshold. For effects that involve only a few jnds, discriminability is prominent in *judged* magnitude (but not in *matched* magnitude—the required task).

The importance of discriminability *per se* can be judged in the control stimuli illustrated in Fig. 5 in which no illusions are intentionally involved. The contrast reversing ring [Fig. 5(b)] is easy to see in the the luminance stimulus and much more difficult to discern in the fullwave control stimulus [Fig. 5(d)]. The optical information (after fullwave rectification of the texture) is the same in both cases.

(4) Choice of stimuli. The Mach bands in second-order Mexican hat stimuli, were of greater magnitude than the first-order Mach bands. In the fullwave-noise textures, the second-order Mach bands were 68% of first-order bands. On the other hand, the fullwave noise peaks and valleys in the Chevreul illusion were actually 40% bigger than the first-order peaks.

Taken together, factors 1, 3 and 4 are (0.78) (0.67) (0.68) = 0.35. These indicate that on a CRT screen, judged magnitude of fullwave-noise Mach band should be 35% of the magnitude of a first-order Mach band. The judged magnitude of the corresponding second-order Chevreul illusion would be 73% of the first-order illusion. In printed versions, these factors probably would be further reduced.

SUMMARY AND CONCLUSIONS

(1) Classical Mach bands were demonstrated in dynamic fullwave stimuli made up of two different carrier textures and a Mach-band modulator: first, a random texture in which the contrast of each pixel of the carrier was chosen randomly and independently to be either +1 or −1; and second, a texture constructed out of center–surround Mexican hats micropatterns that were randomly center-light (+1) or center-dark (−1). Both of these carrier textures, and a uniform homogeneous field were multiplied by a Mach-band modulator. For the second-order stimuli, an induced band of low contrast was perceived at the bottom of the ramp, and a band of high contrast near the top of the ramp. These subjective impressions were quantified by using an interleaved staircase procedure to compare the contrast of a vertical

slice of the Mach band pattern to an adjacent texture bar that varied in contrast from trial-to-trial. The average size of the measured perceptual Mach bands (relative to the neighboring plateaus) was about 3.4% and 5.4% for the two kinds of fullwave stimuli, 5.0% for the luminance stimulus and 0% for the halfwave stimulus.

(2) We also demonstrated Chevreul illusions in a spatially modulated random noise texture (fullwave stimulus). An illusory 'valley' of low contrast was perceived at the foot of each rectangular edge, and an illusory 'hill' of high contrast was perceived atop the lip of each rectangular edge. These subjective impressions were quantified by a nulling procedure. The average size of the measured illusory hills and valleys (relative to the step size) was enormous: about 54% for the fullwave stimulus, and 50% for the luminance stimulus.

(3) Two radially symmetric stimuli were created that exhibited the C–O–C illusion: a first-order luminance stimulus and a second-order fullwave texture stimulus. The magnitude of the illusion (about 7%) was comparable in first- and second-order stimuli.

(4) As in second-order contrast inhibition illusion (Chubb *et al.*, 1989; Cannon & Fullenkamp, 1991, 1993; Singer & D'Zmura, 1994, 1995; Solomon *et al.*, 1993), the illusion is confined to contrast. That is, in the higher contrast areas, the whites were whiter and the blacks blacker, with no change in average brightness. Similarly, in low contrast areas, blacks and whites both gravitate equally towards a neutral gray appearance.

(5) None of these illusions is perceptible in halfwave stimuli, i.e. stimuli that are neutral to Fourier and to fullwave analyses but become equivalent to luminance stimuli after positive or negative halfwave rectification.

(6) Together, these results indicate that the perceptual processes governing second-order spatial interactions, like those governing second-order motion perception (Chubb & Sperling, 1989a, b; Solomon & Sperling, 1994; Lu & Sperling, 1995), reflect fullwave (vs halfwave) rectification. Fullwave interaction was experimentally demonstrated as the modus of the second-order version Simultaneous Brightness Contrast illusion (Chubb *et al.*, 1989). These results are experimental evidence in favor of the type of energy computations (energy is square-law fullwave rectification) proposed by Burr and Morrone to account for these illusions (for a review see Burr & Morrone, 1994).

(7) In the spatial domain, as in motion, second-order processing of contrast-modulated stimuli, after fullwave rectification, is remarkably similar to first-order luminance processing.*

REFERENCES

von Bekesy, G. (1960). Neural inhibitory units of the eye and skin. Quantitative description of contrast phenomena. *Journal of the Optical Society of America, 50*, 1060–1070.

*For recent reviews of theories of first-order Mach bands and Craik–O'Brien–Cornsweet illusions, see Ross *et al.* (1989), Kingdom and Moulden (1992) and Todorovic (1987).

von Bekesy, G. (1968). Mach- and Hering-type lateral inhibition in vision. *Vision Research, 8*, 1483–1499.

Burr, D. C. (1987). Implications of the Craik–O'Brien illusion for brightness perception. *Vision Research, 27*, 1903–1913.

Burr, D. C. & Morrone M. C. (1994). The role of features in structuring visual images. In *Higher-order processing in the visual system.* (Ciba Foundation Symposium 184, pp. 129–146). Chichester: Wiley.

Cannon, M. W. & Fullenkamp, S. C. (1991). Spatial interactions in apparent contrast: Inhibitory effects among grating patterns of different spatial frequencies, spatial positions and orientations. *Vision Research, 31*, 1985–1998.

Cannon, M. W. & Fullenkamp, S. C. (1993). Spatial interactions in apparent contrast: Individual differences in enhancement and suppression effects. *Vision Research, 33*, 1685–1695.

Carlson, C. R. & Klopfenstein, R. W. (1985). Spatial frequency model for hyperacuity. *Journal of the Optical Society of America, A, 2*, 1747–1751.

Carlson, C. R., Anderson, C. H. & Moeller, J. R. (1980). Visual illusions without low spatial frequencies. *Investigative Ophthalmology & Visual Science, 19*, 165–166.

Chevreul, M. E. (1890). *The principles of harmony and contrast of colors* (translated by Martel, C.). London: George Bell and Sons, Bohn's Library.

Chubb, C. & Sperling G. (1989a). Two motion perception mechanisms revealed by distance driven reversal of apparent motion. *Proceedings of the National Academy of Science, U.S.A., 86*, 2985–2989.

Chubb, C. & Sperling, G. (1989b). Second-order motion perception: space/time separable mechanisms. *Proceedings: Workshop on visual motion* (20–22 March, Irvine, Calif.) (pp. 126–138). Washington D.C.: IEEE Computer Society Press.

Chubb, C., Sperling, G. & Solomon, J. A. (1989). Texture interactions determine perceived contrast. *Proceedings of the National Academy of Science, U.S.A., 86*, 9631–9635.

Cornsweet, T. N. (1970). *Visual perception*. New York: Academic Press.

Craik, K. J. W. (1940). Visual adaptation. Doctoral thesis, Cambridge University, Cambridge.

Ercoles, A. M. & Fiorentini, A. (1959). Visibility of the Mach bands as a function of field luminance. *Atti Fond. Giorgio Ronchi, XIV*, 230–235.

Fiorentini, A. & Radici, T. (1958). Brightness, width and position of Mach bands as a function of the rate of variation of the luminance gradient. *Atti Fond. Giorgio Ronchi, XIII*, 145–155.

Fry, G. A. (1948). Mechanism subserving simultaneous brightness contrast. *American Journal of Optometry and Archives of the American Academy of Optometry, 25*, 162–178.

Grossberg, S. & Todorovic, D. (1988). Neural dynamics of 1-D and 2-D brightness perception: A unified model of classical and recent phenomena. *Perception & Psychophysics, 43*, 241–277.

Hartline, H. K. & Ratliff F. (1954). Spatial summation of inhibitory influences in the eye of limulus. *Science, 120*, 781.

Hartwig, E. (1958). Modelluntersuchungen zur quantitativen Erfassung von psysiologischen kontrastfehlern. *Optik, 15*, 414–421.

Huggins, W. H. & Licklider, J. C. R. (1951). Place mechanisms of auditory frequency analysis. *Journal of the Acoustic Society of America, 23*, 290–299.

Kingdom, F. & Moulden, B. (1992). A multi-channel approach to brightness coding. *Vision Research, 32*, 1565–1582.

Kuffler, S. W. (1953). Discharge patterns and functional organization of mammalian retina. *Journal of Neurophysiology, 16*, 37–68.

Legge, G. E. & Foley, J. M. (1980). Contrast masking in human vision. *Journal of the Optical Society of America, 70*, 1458–1471.

Levitt, H. (1971). Transformed up–down methods in psychoacoustics. *Journal of the Acoustical Society of America, 49*, 467–477.

Lowry, E. M. & DePalma, J. J. (1961). Sine-wave response of the visual system. I. The Mach phenomenon. *Journal of the Optical Society of America, 51*, 740–746.

Lu, Z.-L. & Sperling, G. (1995). The functional architecture of human visual motion perception. *Vision Research, 35*, 2697–2722.

Mach, E. (1865). Ueber die Wirkung der raumlichen Vertheilung des

Lichtreizes auf die Netzhaut. *I.S.-B. Akad. Wiss. Wien. math.-nat. Kl., 54*, 303–322. (Translated by Ratliff, 1965.)

McCollough, C. (1955). The variation in width and position of Mach bands as a function of luminance. *Journal of Experimental Psychology, 49*, 141–152.

Morrone, M. C., Burr, D. C. & Ross, J. (1994). Illusory brightness step in the Chevreul illusion. *Vision Research, 34*, 1567–1574.

Nachmias, J. & Sansbury, R. V. (1974). Grating contrast: Discrimination may be better than detection. *Vision Research, 14*, 1039–1042.

O'Brien, V. (1958). Contour perception, illusion, and reality. *Journal of the Optical Society of America, 48*, 112–119.

Ratliff, F. (1965). *Mach bands*. San Francisco, Calif.: Holden-Day.

Ross, J., Holt, J. J. & Johnstone, J. R. (1981). High frequency limitations on Mach bands. *Vision Research, 21*, 1165–1167.

Ross, J., Morrone, M. C. & Burr, D. C. (1989). The conditions under which Mach bands are visible. *Vision Research, 29*, 699–715.

Singer, B. & D'Zmura, M. (1994). Color contrast induction. *Vision Research, 34*, 3111–3126.

Singer, B. & D'Zmura, M. (1996). Contrast gain control: A bilinear model for chromatic selectivity. *Journal of the Optical Society of America, A*. In press.

Solomon, J. A. & Sperling, G. (1994). Full-wave and half-wave rectification in second-order motion perception. *Vision Research, 34*, 2239–2257.

Solomon, J. A., Sperling, G. & Chubb, C. (1993). The lateral inhibition of perceived contrast is indifferent to on-center/off-center segregation but specific to orientation. *Vision Research, 33*, 2671–2683.

Sperling, G. (1964). Linear theory and the psychophysics of flicker. *Documenta Ophthalmologica, 18*, 3–15.

Sperling, G. (1989). Three stages and two systems of visual processing. *Spatial Vision, 4*, 183–207.

Stromeyer, C. F. & Klein, S. (1974). Spatial frequency channels in human vision as asymmetric (edge) mechanisms. *Vision Research, 14*, 1409–1420.

Taylor, W. K. (1956). Electrical simulation of some nervous system function activities. In Cherry, C. (Ed.), *Information theory*. New York: Academic Press.

Todorovic, D. (1987). The Craik–O'Brien–Cornsweet effect: New Varieties and their theoretical implications. *Perception & Psychophysics, 42*, 545–560.

Watt, R. J. & Morgan, M. J. (1985). A theory of the primitive spatial code in human vision. *Vision Research, 25*, 1661–1674.

Wilson, H. R., Ferrera, V. P. & Yo, C. (1992). A psychophysically motivated model for two-dimensional motion perception. *Visual Neuroscience, 9*, 79–97.

Acknowledgement—Supported by AFOSR, Life Sciences, Visual Information Processing Program.